

## Redox States of Long Oligothiophenes: Two Polarons on a Single Chain

John A. E. H. van Haare, Edsko E. Havinga, Joost L. J. van Dongen, René A. J. Janssen,\* Jérôme Cornil, and Jean-Luc Brédas

**Abstract:** A detailed investigation is presented of the redox states of three oligothiophenes ( $nT$ ) with 6, 9, and 12 thiophene units. While open-shell radical cations (polarons) and closed-shell dicationic (bipolarons) are usually invoked as the primary redox species in these systems, we have obtained evidence that the dication of the longest oligothiophene (12T) has an electronic structure with two individual polarons. The redox states of 6T, 9T, and 12T have been fully characterized using UV/visible/near-IR and ESR spectroscopy in

combination with electrospray mass spectrometry. For 6T and 9T, single-electron oxidation in dichloromethane produces the corresponding radical cations, which form spinless  $\pi$  dimers at lower temperatures. A second oxidation step forms dicationic species which possess a bipolaronic electronic structure. However, the redox behavior of the longest

oligothiophene, 12T, is entirely different. Radical cations of 12T disproportionate into neutral oligomers and dicationic species, except at the lowest oxidation levels. The spectral data for doubly oxidized 12T are incompatible with those expected for a bipolaronic structure but are consistent with the formation of two individual polarons on a single chain; this interpretation is also supported by the results from correlated quantum chemical calculations.

**Keywords:** conducting materials • oligomers •  $\pi$  interactions • radical ions • redox chemistry

### Introduction

$\pi$ -conjugated polymers attract considerable attention as functional materials in a variety of (opto)electronic devices, such as light-emitting diodes, field-effect transistors, lightweight batteries, solar cells, and electrochromic devices.<sup>[1, 2]</sup> In their pristine form these polymers are semiconductors with a band gap in the range of approximately 1.5–3.5 eV. One of the most important features of  $\pi$ -conjugated polymers is their ability to become highly conducting after oxidative or reductive doping. Many of the applications foreseen for these materials are associated with some kind of charge transport, albeit at greatly varying doping levels. Therefore, the nature of the charge carriers in these materials as a function of the degree of doping has been one of the focal points of interest since the discovery of high levels of electrical conductivity.<sup>[3–9]</sup>

The first step in oxidative (or reductive) doping of the conjugated polymer is the formation of a radical cation (or anion); depending on the Coulomb potential from the associated counterion, the charge can move along the  $\pi$ -conjugated chain. These radical ions, often designated as polarons,<sup>[10]</sup> are considered to be self-localized charged species because, even for long chains, the geometrical change associated with the oxidation (or reduction) is confined to a limited number of monomeric units. As a result of the characteristic strong coupling of the electronic structure with the geometric structure for  $\pi$ -conjugated materials (electron–lattice coupling),<sup>[6]</sup> this deformation causes new electronic states to appear within the  $\pi$ – $\pi^*$  band gap of the polymer. For a positive polaron (radical cation) a singly occupied level is generated above the valence band in the  $\pi$ – $\pi^*$  band gap and an empty level appears below the conduction band.<sup>[6]</sup> Initially, the positive polaron was characterized as exhibiting three electronic absorptions, associated with a transition from the top of the valence band to the singly occupied polaron level, one between the two polaron levels, and a transition from the occupied polaron level to the conduction band.<sup>[6]</sup> Because of the single occupancy of the highest occupied energy level, the polaron has an associated ESR signal. With increasing doping levels, a situation is created where more than one charge is removed from a single chain. It has been argued that, as a result of the strong electron–lattice interaction, two polarons on a single chain coalesce into a bipolaron, which is a doubly charged spinless

[\*] Dr. R. A. J. Janssen, Dr. J. A. E. H. van Haare, Dr. E. E. Havinga, J. L. J. van Dongen  
Laboratory of Organic Chemistry  
Eindhoven University of Technology  
P.O. Box 513, NL-5600 MB Eindhoven (The Netherlands)  
Fax: (+31)40-2451036  
E-mail: tgorj@chem.tue.nl  
Dr. J. Cornil, Prof. J. L. Brédas  
Service de Chimie des Matériaux Nouveaux  
Centre de Recherche en Electronique et Photonique Moléculaires  
Université de Mons-Hainaut  
Place du Parc 20, B-7000 Mons (Belgium)

deformation on a  $\pi$ -conjugated chain.<sup>[11]</sup> Although two like charges are part of the same chain deformation in a bipolaron, the energy gained by forming only one deformation may outweigh the increased Coulomb repulsion energy.<sup>[6]</sup> Important support for the generation of bipolarons is provided by the loss of the ESR signal at higher doping levels, which is observed for almost all  $\pi$ -conjugated materials. On the other hand, the electronic spectra of bipolarons have raised a number of questions. Initially, it was found in conjugated polymers that the transition from polarons to bipolarons at higher doping levels led to a suppression of the transition between the two in-gap levels and that the remaining two absorptions shifted to higher energies. The two absorptions of a positive bipolaron have been attributed to excitations from the valence band to the empty first and second bipolaron levels. The hypsochromic shift can be rationalized by the stronger lattice deformation of a bipolaron as compared to a polaron, which causes the electronic states appearing in the gap to be further away from the band edges.<sup>[6]</sup> Although it was found experimentally that the two transitions have rather similar intensity, the model developed by Fesser, Bishop, and Campbell (FBC model)<sup>[5]</sup> predicts that the second transition should be far less intense, so there is a marked discrepancy between theory and experiment.<sup>[12]</sup>

This situation has been considerably clarified by oxidation experiments on  $\pi$ -conjugated oligomers with a well-defined conjugation length as model compounds for polymers. One of the key examples in this respect was reported by Garnier et al. for sexithiophene, which exhibits only two electronic absorptions for the radical cation and only one strong absorption for the dication.<sup>[13]</sup> In recent years various experimental and theoretical studies have provided a detailed and coherent insight into the characteristics of the first two oxidation states of oligothiophenes with a limited number of rings.<sup>[14–22]</sup> The first oxidation potential of oligothiophenes in dilute solution decreases with chain length and exhibits an almost linear relationship with the inverse number of thiophene rings ( $1/n$ ). In the first oxidation wave, one electron is removed and a radical cation (also referred to as a positive polaron by analogy with condensed matter physics terminology: a positive polaron is defined as a radical cation associated to a local geometry relaxation<sup>[6]</sup>) is formed which exhibits an ESR signal and two subgap electronic absorptions that increase in intensity with the number of oxidized oligomers at the cost of the  $\pi$ – $\pi^*$  transition of the neutral  $n$ T oligomer. Semiempirical AM1 calculations reveal that a geometry deformation of the aromatic rings occurs in the radical cation to a semiquinoidic structure.<sup>[22]</sup> The spatial extension of this deformation, which is located at the center of the chain, is estimated to be five units or less without considering the presence of counter ions. At higher oxidation potentials, the oligothiophene radical cation can be converted to the corresponding dication. The second oxidation potential decreases with chain length, with a steeper slope than that of the first oxidation. Hence, the potential difference between subsequent redox states decreases for longer oligomers as a result of a decreasing Coulombic repulsion between the two charges. The short-chain oligothiophene dications have a single, strong, subgap electronic absorption and no ESR signal. The

AM1-optimized geometries of the oligothiophene dications indicate the formation of a positive bipolaron, since the two like charges are associated to a strong quinoidic deformation at the center of the molecule. The amplitude of the defect progressively diminishes when going from the center to the end of the molecule. The upper limit for the width of the bipolaron geometry relaxation, as estimated from the AM1 calculations, corresponds to nine thiophene units.<sup>[22]</sup>

It has been demonstrated that radical cations of oligothiophenes have a tendency to form  $\pi$  dimers reversibly in solution at high concentrations or low temperatures.<sup>[14, 15]</sup> Although the geometry of such a  $\pi$  dimer is not exactly known, they are envisaged as a face-to-face complex of two radical cations interacting through their  $\pi$  orbitals. This view is corroborated by a recent X-ray crystallographic study of a radical cation of a substituted terthiophene.<sup>[16]</sup> The face-to-face interaction of the singly occupied, degenerate  $\pi$  orbitals of the two constituent radical cations results in a splitting into two new energy levels and a net energy gain when the lower of these new energy levels becomes doubly occupied. This gain in energy provides the driving force for the formation of a  $\pi$  dimer and opposes the increased Coulomb repulsion, which results from combining two like-charged species in a single complex. The  $\pi$ -dimerization of radical cations, being the result of a fine balance between attractive and repulsive interactions, is strongly dependent on the solvent and the nature of the counterions.<sup>[23]</sup>  $\pi$  Dimers are ESR-silent, and because they possess two electronic absorptions in the  $\pi$ – $\pi^*$  gap at somewhat higher energy than the corresponding radical cations it has been suggested that  $\pi$  dimers are a likely alternative to bipolarons as the predominant charge carriers in heavily doped conjugated polymers.<sup>[24]</sup> In addition to oligothiophenes,  $\pi$  dimers have been identified for radical cations of oligopyrroles and oligo(*p*-phenylene vinylenes).<sup>[25, 26]</sup>

Although  $\pi$  dimers could be formed in conjugated polymers as a result of complexation of different chains or chain segments, the situation for a multiply charged single chain remains unclear.<sup>[9]</sup> The oligomers that have been studied in detail up to now have a rather limited conjugation length,<sup>[13–18, 27]</sup> and far less attention has been paid to longer systems.<sup>[19, 20, 28, 29]</sup> However, conjugation length is an important parameter in differentiating between the various electronic states. For a short oligomer molecule, there is a limit to the decrease in Coulomb repulsion of two like charges, because they cannot diffuse further apart than the limited length of the conjugated system. For a long oligomer (or an infinite polymer), however, the situation is different because there is no restriction in moving the two charges apart (provided the counterions are fully mobile). The decrease in Coulomb repulsion energy that is obtained by moving the two like charges apart on a single chain may outweigh the concurrent energy cost that results from the fact that the two charges no longer share the same geometrical deformation.<sup>[30]</sup> Hence, a transition between a bipolaron and two isolated polarons, as energetically favored structure, could occur as a function of chain length, as has been predicted on the basis of semiempirical calculations.<sup>[31]</sup>



the energy of the subgap absorptions evolve in a linear fashion with  $1/n$ , in good agreement with experimental data.

**Bipolarons:** Next, we consider an oligothiophene dication with an electronic configuration that corresponds to a bipolaron, that is, one geometry deformation on the chain as for a polaron. In a bipolaron the  $a_u$  HOMO level is doubly occupied and the electronic state is of  $1^1A_g$  symmetry. The transition from the  $a_u$  HOMO level to the lowest empty bipolaron  $b_g$  level ( $b_g \leftarrow a_u$ ) is strongly dipole allowed and polarized along the long axis of the molecule. Many dications of  $\pi$ -conjugated oligomers show this transition as a single intense absorption well below the  $\pi$ - $\pi^*$  band gap, usually located between the two subgap absorptions of the radical cation.<sup>[34]</sup> In a one-electron description, this excitation originates from the near-IR band of the radical cation, but has shifted to higher energy as a result of the greater geometrical deformation that occurs in a bipolaron in comparison with a polaron. The strong coupling of the electronic structure with the geometrical structure pulls the unoccupied  $b_g$  orbital further into the band gap, which moves the excitation to higher energies. Theoretical calculations fully confirm this description.<sup>[21, 22]</sup>

**Two polarons on a chain:** Finally, we consider a long oligothiophene carrying two charges which are confined to two different geometrical deformations (A and B) near each end of the molecule. The molecular orbitals that observe the overall molecular symmetry, must be described with symmetric ( $\phi_+$ ,  $a_u$ ) and antisymmetric ( $\phi_-$ ,  $b_g$ ) linear combinations of the two wavefunctions ( $\phi_A$  and  $\phi_B$ ) describing the individual radical cations (Figure 3), as described in Equations (1) and (2), where  $S_{AB}$  is the overlap of the wavefunctions  $\phi_A$  and  $\phi_B$ .

$$\phi_+ = (2 + 2S_{AB})^{-1/2} (\phi_A + \phi_B) \quad (1)$$

$$\phi_- = (2 - 2S_{AB})^{-1/2} (\phi_A - \phi_B) \quad (2)$$

When the interaction between the radical cations ( $\phi_A$  and  $\phi_B$ ) is small,  $\phi_+$  and  $\phi_-$  are almost degenerate, and the electronic configuration of the two radical cations (two polarons) on the single chain cannot be described with a single determinant wavefunction but must involve configuration interaction. Following Borden, we consider a diradical containing a

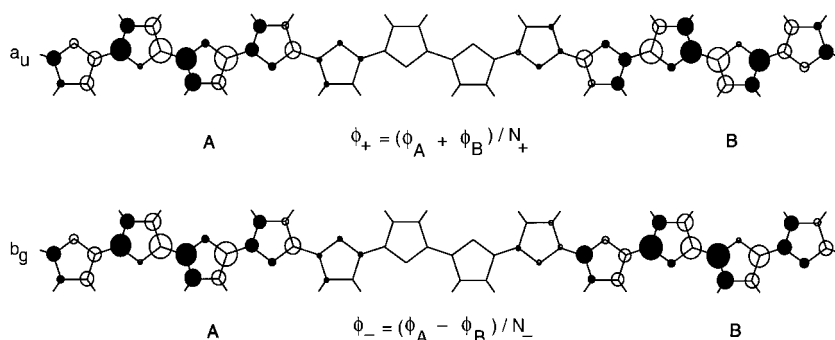


Figure 3. Schematic representation of the frontier  $\pi$  orbitals (top view) of the symmetrized two-polaron wavefunctions of duodecithiophene. The shading indicates the phase of the molecular orbitals.

symmetry element such that the two highest relevant MOs ( $\phi_+$  and  $\phi_-$ ) belong to different irreducible representations, that is, behave differently with respect to at least one symmetry operation.<sup>[35, 36]</sup> In principle, six electronic configurations can be distinguished when placing two electrons in two MOs ( $\phi_+$  and  $\phi_-$ ). Three of these configurations form the  $M_s = -1, 0,$  and  $+1$  components of the same triplet state. Of the three remaining singlet configurations, only the two closed-shell configurations mix, giving rise to two  $1^1A_g$  states. The third singlet state does not mix due to the different spatial symmetry of  $\phi_+$  and  $\phi_-$ . To summarize, the six configurations give rise to the following four low-lying states that can be described with Equations (3)–(6).<sup>[37]</sup>

$$1^1A_g \quad \Psi_1 = c_1 |\phi_+ \bar{\phi}_+| - c_2 |\phi_- \bar{\phi}_-| \quad (3)$$

$$2^1A_g \quad \Psi_2 = c_2 |\phi_+ \bar{\phi}_+| + c_1 |\phi_- \bar{\phi}_-| \quad (4)$$

$$1^3B_u \quad \Psi_3 = \{ |\phi_+ \bar{\phi}_-| + |\bar{\phi}_+ \phi_-| \} / \sqrt{2} \quad M_s = 0 \text{ component} \quad (5)$$

$$1^1B_u \quad \Psi_4 = \{ |\phi_+ \bar{\phi}_-| - |\bar{\phi}_+ \phi_-| \} / \sqrt{2} \quad (6)$$

The off-diagonal element in the matrix that describes the mixing of the two closed-shell  $1^1A_g$  configurations  $|\phi_+ \bar{\phi}_+|$  and  $|\phi_- \bar{\phi}_-|$  is the exchange integral  $K_{+-}$ . In the limit that the two radical cations have a negligible interaction, the symmetrized polaron wavefunctions  $\phi_+$  and  $\phi_-$  are degenerate and the mixing of the  $|\phi_+ \bar{\phi}_+|$  and  $|\phi_- \bar{\phi}_-|$  configurations will be complete, resulting in  $c_1 = c_2 = 1/\sqrt{2}$ . With an increasing distance between the two polarons on a long chain, the energy difference between the  $1^1A_g$  and  $1^3B_u$  states, which describe the spin states of a diradical on a single chain, decreases and at a certain point the singlet and triplet states become degenerate.<sup>[37]</sup> Similarly, the energy difference between the two higher lying states  $2^1A_g$  and  $1^1B_u$  disappears. In this limit, the energy difference between the  $1^1A_g/1^3B_u$  states and the  $2^1A_g/1^1B_u$  states is equal to  $2K_{+-}$ .<sup>[38]</sup>

From these considerations it appears that both the bipolaron, with a single geometrical deformation, and the two-polaron configuration, with two separate geometry distortions, correspond to the  $1^1A_g$  state described by Equation (3). The crucial difference between the two possible configurations, however, is the relative magnitude of the coefficients  $c_1$  and  $c_2$ . In a bipolaron, the coefficients will differ substantially (i.e.  $c_1 \gg c_2$ ), while for two individual, non-interacting, polarons the coefficients will be similar (i.e.  $c_1 \approx c_2$ ).

Having addressed the electronic wavefunction of the two-polaron state, we consider the dipole-allowed transitions that originate from it. Within the  $C_{2h}$  point group a  $1^1B_u \leftarrow 1^1A_g$  excitation is dipole-allowed, and because it is polarized along the long axis of the molecule, it is expected to be strong. In a one-electron description several single excitations that correspond to either a  $b_g \leftarrow a_u$  or a  $a_u \leftarrow b_g$  electronic transition may give rise to a  $1^1B_u$  state (Figure 2). Many of these transitions are closely related to the two

transitions that would occur in an isolated radical cation. In addition, however, a transition might occur that involves an electron transfer from one radical cation to the other, corresponding to single excitation among the  $\phi_+$  and  $\phi_-$  orbitals (i.e.  $\phi_+ \leftarrow \phi_-$  or  $\phi_- \leftarrow \phi_+$ ) (Figure 2). This transition results in the  $^1B_u$  state described by Equation (6). In the limit of two noninteracting polarons, the excitation energy of this transition will be equal to  $2K_{+-}$ .<sup>[38]</sup> Whether this qualitative picture of the optical transitions is correct remains to be tested experimentally and confirmed with high-level calculations. Moreover, since a range of close-lying  $^1B_u$  configurations can be reached from the  $^1A_g$  ground state by  $b_g \leftarrow a_u$  and  $a_u \leftarrow b_g$  excitations, it can be expected that configurational mixing occurs among the various  $^1B_u$  configurations, so that an ordering of the  $^1B_u$  states cannot be predicted by simple arguments.

## Results

In order to allow for a direct comparison of the redox properties of 6T, 9T, and 12T, we briefly summarize and reconsider some of the results previously obtained for unsubstituted and dodecyl-substituted 6T as described by Garnier et al.<sup>[13]</sup> and Bäuerle et al.<sup>[17]</sup>

**Didodecyl sexithiophene (6T):** The cyclic voltammogram of 6T recorded in dichloromethane (Figure 4a) shows two consecutive chemically reversible oxidation waves at  $E_1^o = 0.81$  and  $E_2^o = 1.03$  V vs. SCE, in good agreement with values reported by Bäuerle et al.<sup>[17]</sup> The distance between the anodic and cathodic peaks is about 90 mV.

Figure 5 shows the evolution of the UV/visible/near-IR spectrum of a 6T solution upon oxidation by addition of small aliquots of a solution of thianthrenium perchlorate in dichloromethane. Thianthrenium perchlorate ( $\text{THI}^{+\cdot}\text{ClO}_4^-$ )

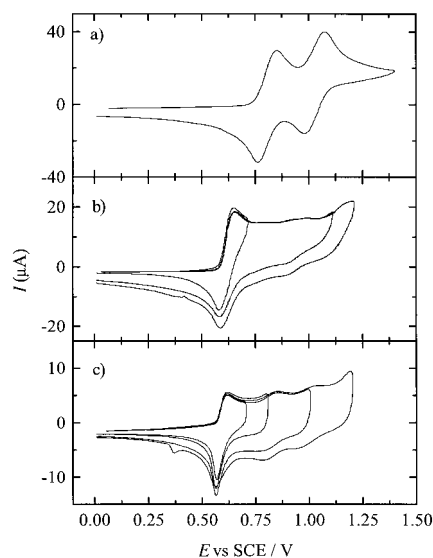


Figure 4. Cyclic voltammograms of a) 6T; b) 9T; c) 12T at  $10^{-3}$  M concentration recorded in dichloromethane/TBAH (0.1 M) at  $T = 295$  K, scan rate  $100 \text{ mV s}^{-1}$ , potential vs. SCE calibrated against  $\text{Fc}/\text{Fc}^+$  (0.47 V).

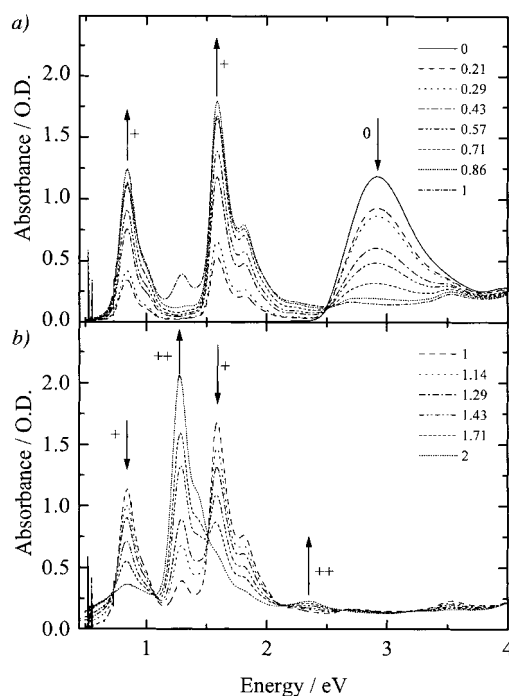


Figure 5. Evolution of the UV/visible/near-IR spectra of a  $2.5 \times 10^{-5}$  M solution of 6T in dichloromethane at  $T = 295$  K during conversion a) from neutral 6T to the  $6\text{T}^{+\cdot}$  radical cation and b) from  $6\text{T}^{+\cdot}$  to  $6\text{T}^{2+}$  dication, resulting from the addition of aliquots of a  $3 \times 10^{-4}$  M solution of  $\text{THI}^{+\cdot}\text{ClO}_4^-$  in dichloromethane. The inset shows the number of equivalents of  $\text{THI}^{+\cdot}\text{ClO}_4^-$  added.

was chosen as the oxidizing agent for the present studies because it combines a relatively high oxidation potential of  $E^o = 1.23$  V vs. SCE with characteristic signals in the UV/visible spectrum ( $E = 2.23$  and  $4.25$  eV) and the ESR spectrum ( $g = 2.0081$ ,  $a(\text{H}) = 0.132$  mT).<sup>[39, 40]</sup> The appearance of these signals in the electronic or ESR spectra indicates that further addition of  $\text{THI}^{+\cdot}$  does not result in (complete) oxidation of oligothiophene. As an additional advantage, the thianthrene formed in the reduction reaction absorbs at  $E = 4.83$  eV, well outside the region of interest for the redox states of the present oligothiophenes. Figure 5a represents the oxidation of neutral 6T ( $E = 2.92$  eV) to the corresponding  $6\text{T}^{+\cdot}$  radical cation.  $6\text{T}^{+\cdot}$  exhibits two strong absorption bands at  $E = 1.59$  and  $0.84$  eV, each accompanied by a vibronic transition at higher energy (at  $E = 1.81$  and  $\sim 1.0$  eV, respectively). The band at  $1.59$  eV is assigned to an excitation from the singly occupied polaron level to the LUMO ( $a_u \leftarrow b_g$ ), whereas the band at  $0.84$  eV is attributed to an excitation from the highest doubly occupied MO to the first polaron level ( $b_g \leftarrow a_u$ ), as shown in Figure 2 (see Theory section). In addition a third, weak, band at  $3.55$  eV is found that seems to be associated with  $6\text{T}^{+\cdot}$ . The isobestic point at  $E = 1.50$  eV indicates the interconversion of two species, consistent with the oxidation of 6T into  $6\text{T}^{+\cdot}$ .

These spectral data of  $6\text{T}^{+\cdot}$  are in excellent agreement with the electronic spectra of  $6\text{T}^{+\cdot}$  obtained by doping with ferric chloride<sup>[17]</sup> or by excited-state electron transfer,<sup>[41]</sup> and are fully supported by the VEH-calculated transition energies at  $0.93$  and  $1.47$  eV.<sup>[21]</sup> The results also correspond remarkably well to the spectra of  $6\text{T}^{+\cdot}$  observed in photoinduced

absorption (PIA) experiments on thin films<sup>[42]</sup> and in field-induced charging of semitransparent metal–insulator–semiconductor devices, where counterions are absent.<sup>[43]</sup> With respect to the third, low-intensity, absorption at 3.55 eV for  $6T^{+}$ , it is interesting to note that correlated calculations performed on short oligo(*p*-phenylene vinylene)s indicate that a positive polaron is characterized not only by two strong subgap absorption features, but also by a third weak absorption peak at an energy higher than that of the neutral band.<sup>[44]</sup> On the basis of this result, the weak band of  $6T^{+}$  may be the consequence of a mixing of formally forbidden excitations, whose main contributions originate from transitions between the singly occupied polaron level ( $b_g$ ) and the LUMO + 1 ( $b_g$ ) and between the highest doubly occupied level ( $a_u$ ) and LUMO ( $a_u$ ) (Figure 2).

Upon further oxidation, the radical cation is converted to the  $6T^{2+}$  dication (Figure 5b), which exhibits a strong absorption at  $E = 1.28$  eV together with a shoulder at  $E = 1.42$  eV and a second, much smaller, band at  $E = 2.35$  eV. In addition to the loss of signals at  $E = 0.84$ , 1.59, and 3.55 eV, the transformation of  $6T^{+}$  into  $6T^{2+}$  is characterized by a series of isosbestic points ( $E = 0.73$ , 1.07, 1.50, 2.12, and 2.62 eV). The experimental data for  $6T^{2+}$  are in agreement with the model outlined in the Theory section (Figure 2) and quantum chemical calculations; the lowest optical feature of the dication is calculated at 1.08 eV at the VEH level and is described by the symmetry-allowed transition taking place between the HOMO level ( $a_u$ ) and the lowest bipolaron level ( $b_g$ ).<sup>[21]</sup> The weak absorption band of the dication at 2.35 eV, which was first noticed by Horowitz et al.,<sup>[19]</sup> can be assigned to the normally forbidden one-electron excitation between the HOMO ( $a_u$ ) and the highest bipolaron level ( $a_u$ ), estimated at 2.02 eV by the VEH method; this band can appear in the spectrum due to some symmetry lowering in solution and breakdown of the selection rules. The results of these chemical oxidations are once again supported by the optical spectra of  $6T^{2+}$  obtained by photoinduced and field-induced charging.<sup>[42, 43]</sup>

It is important to note that the 220 mV separation between the first and second oxidation potential of 6T is large enough to preclude the simultaneous presence to any significant extent of the three redox states  $6T$ ,  $6T^{+}$ , and  $6T^{2+}$  in dichloromethane solution. After reduction with an excess of hydrazine monohydrate at either the  $6T^{+}$  or  $6T^{2+}$  levels of oxidation, the original UV/visible/near-IR spectrum of 6T is recovered, demonstrating the stability and complete reversibility of the first two one-electron oxidations of 6T.

These optical studies and their assignments are fully consistent with the observed ESR spectrum of  $6T^{+}$  (Figure 6) and the evolution of the doubly integrated ESR intensity with progressing oxidation level (Figure 7). By measuring ESR and UV/visible/near-IR spectra in a single cell under identical conditions, we confirmed that the UV/visible/near-IR spectrum of  $6T^{+}$ , shown in Figure 5a, reaches maximum intensity at the oxidation level for which the ESR intensity is the highest. Further oxidation results in the complete loss of the ESR spectrum, when  $6T^{+}$  is fully converted to  $6T^{2+}$ , in accordance with the diamagnetic character of the dication (Figure 7).<sup>[13, 17]</sup>

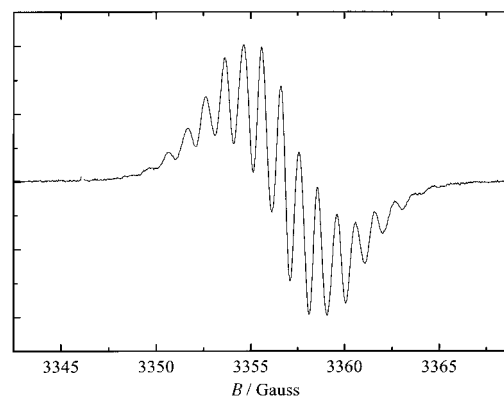


Figure 6. ESR spectrum of the  $6T^{+}$  radical cation in dichloromethane at  $T = 295$  K. The ESR spectrum is characterized by  $g = 2.0022$  and can be successfully simulated using the following hyperfine coupling parameters:  $a(H) = 0.193$  mT (4H);  $a(H) = 0.125$  mT (2H);  $a(H) = 0.106$  mT (2H);  $a(H) = 0.097$  mT (2H);  $a(H) = 0.090$  mT (2H);  $a(H) = 0.075$  mT (2H);  $a(H) = 0.011$  mT (2H).

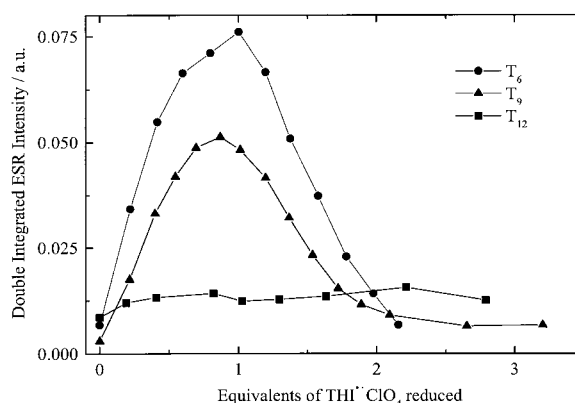


Figure 7. Evolution of the double integrals of the ESR signal recorded for 6T, 9T, and 12T as a function of the number of equivalents of  $THI^{+}ClO_4^{-}$  being reduced to THI.

Direct analysis of the oxidized 6T solutions with ESMS gives information on the ions present in solution. It is important to note that the relative intensity of the peaks at different  $m/z$  values does not necessarily correlate with the relative concentration of the various charged species present in solution as deduced from the optical absorption and ESR experiments. This is a result of the different response for different ions and the possibility of subsequent redox reactions in the course of the ionization process in the ES mass spectrometer. The ES mass spectrum of an oxidized sample of 6T (converted to  $6T^{+}$  for about 75% as judged from UV/visible/near-IR and ESR) is shown in Figure 8. The strongest peak is observed at  $m/z = 830.5$  amu resulting from the  $6T^{+}$  radical cation (calcd  $m/z = 830.3$  amu), while traces of other oligomers are detected (Figure 8).<sup>[45]</sup> The isotope distribution of the  $m/z = 830.5$  amu peak possesses unit amu mass separation, confirming the single charge. At  $m/z = 415.5$  amu (i.e., half the  $m/z$  value of  $6T^{+}$ ), the  $6T^{2+}$  dication is observed, exhibiting an isotope mass separation of 0.5 amu units, consistent with the twofold charge.

At higher  $m/z$  values than that of  $6T^{+}$ , two small peaks are detected. The first peak at  $m/z = 1660.6$  amu corresponds to a

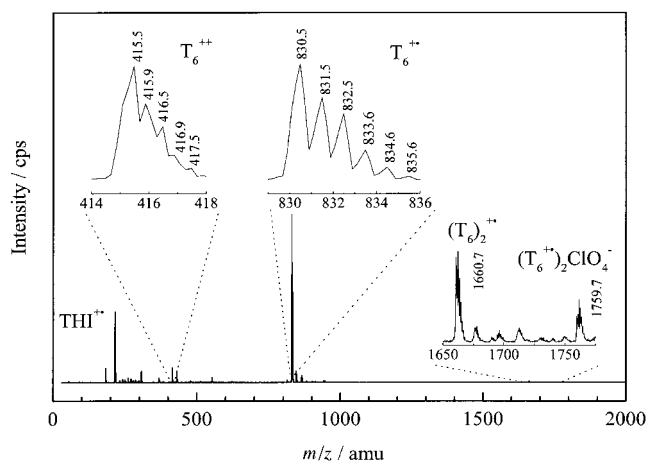


Figure 8. ES mass spectrum of a dichloromethane solution of the  $6T^+$  radical cation fed directly into the ES mass spectrometer. The insets show expanded regions of interest (see text). The signals at  $m/z = 184.1$ ,  $216.1$ , and  $431.1$  amu are caused by  $THI^+ - S$ ,  $THI^+$ , and  $(THI)_2^+$  respectively. Small impurities are present at  $m/z = 1244.6$  amu ( $9T^+$ ),  $m/z = 553.3$  amu ( $12T^{3+}$ ), and  $m/z = 864.3$  amu ( $\alpha\text{-Cl-}6T^+$ ).<sup>[45]</sup>

singly charged complex of two  $6T$  molecules (i.e.  $(6T)_2^+$ , calcd  $m/z = 1660.6$  amu),<sup>[46]</sup> which can be considered as a charge-transfer complex of a  $6T^+$  radical cation with a neutral  $6T$  molecule.<sup>[47]</sup> Similar dimer radical cations  $[(nT)_2^+]$  have been reported to be formed in films of methyl end-capped oligothiophenes.<sup>[48]</sup> The  $(6T)_2^+$  peak at  $m/z = 1660.6$  amu was no longer observed when neutral  $6T$  was fully converted to the radical cation. The second peak at  $m/z = 1759.7$  amu is assigned to a complex of two  $6T^+$  radical cations and a perchlorate anion (calcd  $m/z$  for  $[(6T)_2ClO_4]^+$  is  $1759.6$  amu). Although the exact nature of the bonding in this complex cannot be deduced from the ESMS data, we tentatively assign this complex to a  $\pi$  dimer of two  $6T^+$  radical cations with a perchlorate counterion, based on the well-known dimerization behavior of oligothiophene radical cations in solution at low temperatures.<sup>[24]</sup> A MS–MS analysis of this peak gave a signal at  $m/z = 830.5$  amu and no peak in the negative mass spectrum, consistent with a dissociation into  $6T^+$  and  $6TClO_4$ . The parent peak of  $(6T)_2^+$   $\pi$  dimers is expected to coalesce with that of the  $6T^+$  signal at  $m/z = 830.5$  amu, however, indicates that this is largely due to  $6T^+$  radical cations and gives no evidence of the presence of  $\pi$  dimers, which should have a  $0.5$  amu separation.

The changes in ESR and in the electronic spectrum of  $6T^+$  with temperature have been described in great detail by Bäuerle et al.<sup>[17]</sup> and will not be repeated here. Our experiments confirm that in the temperature range of  $295\text{--}220$  K a fully reversible  $\pi$  dimerization of the  $6T^+$  radical cations occurs to a diamagnetic state, according to Equation (7).



The  $(6T)_2^+$   $\pi$  dimer shows two dominant electronic absorptions at  $E = 1.12$  and  $1.97$  eV that are significantly blue-shifted with respect to those of the isolated species. The dimerization equilibrium of Equation (7) is characterized by

isosbestic points at  $E = 0.99$  and  $1.75$  eV.<sup>[49]</sup> From the changes in the optical absorption spectra and, independently, from the reduction of the doubly integrated ESR signal intensity, the dimerization enthalpy of  $6T^+$  has been determined as  $\Delta H_{\text{dim}}^0 = -43 \pm 7$  kJ mol<sup>-1</sup>, which is less than the value of  $\Delta H_{\text{dim}}^0 = -87 \pm 16$  kJ mol<sup>-1</sup> previously reported.<sup>[17, 50]</sup>

**Tridodecyl nonithiophene (9T):** The cyclic voltammogram of 9T (Figure 4b) is more complex than that of 6T, where two reversible waves are obtained. For 9T, the first oxidation wave at  $E^\circ = 0.62$  V vs. SCE is chemically fully reversible if the voltage scan is reversed before  $E = 0.75$  V. The distance between anodic and cathodic peaks is  $70$  mV. Extending the sweep to higher potentials gives two to three ill-resolved quasireversible broad waves. This complicated behavior in cyclic voltammetry may have its origin in various effects, namely, 1) adsorption or precipitation of charged species; 2) interactions between electroactive centers such as the formation of  $\pi$  dimers at the electrode even at room temperature; 3) conformational changes or the fact that a mixture of regioisomers is used; or 4) slow electron transfer.<sup>[51]</sup>

The chemical oxidation of 9T has been monitored with UV/visible/near-IR spectroscopy in detail (Figure 9). Upon addition of  $THI^+ClO_4^-$ , the band of neutral 9T at  $E = 2.75$  eV is

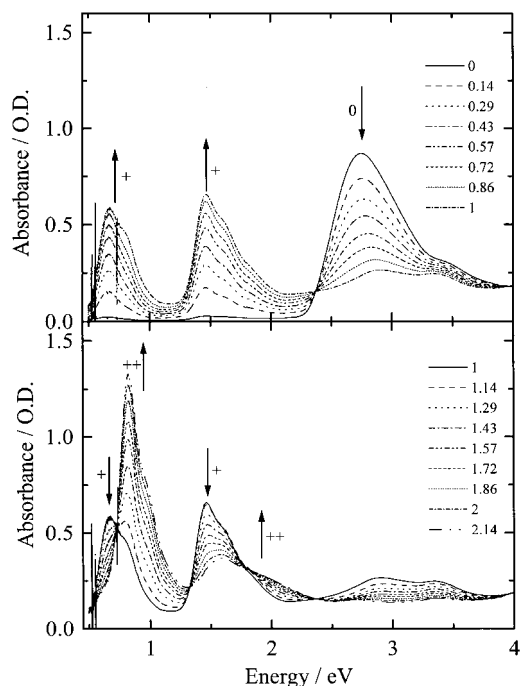


Figure 9. Evolution of the UV/visible/near-IR spectra of a  $1.2 \times 10^{-5}$  M solution of 9T in dichloromethane at  $T = 295$  K during conversion from neutral 9T to the  $9T^+$  radical cation (top) and from  $9T^+$  to  $9T^{2+}$  dication (bottom) resulting from the addition of aliquots of a  $3 \times 10^{-4}$  M solution of  $THI^+ClO_4^-$  in dichloromethane. The inset shows the number of equivalents of  $THI^+ClO_4^-$  added.

replaced by two new bands at  $E = 1.46$  and  $0.67$  eV of the  $9T^+$  radical cation. The high-energy band of  $9T^+$  has an additional vibronic transition as a shoulder at approximately  $E = 1.61$  eV. The low-energy band contains a broad tail to higher energy that possibly contains unresolved vibronic coupling. The

bands at 1.46 and 0.67 eV are assigned to excitations from the singly occupied polaron level ( $a_2$ ) to the LUMO ( $b_2$ ) and from the highest doubly occupied level ( $b_2$ ) to the singly occupied polaron level ( $a_2$ ) (see Theory section, Figure 2). The conversion of 9T into  $9T^{+\cdot}$  results in an isosbestic point at  $E = 2.37$  eV. Upon further oxidation to  $9T^{2+\cdot}$ , the two bands of  $9T^{+\cdot}$  are replaced by a strong absorption at  $E = 0.82$  eV with a vibronic shoulder at  $E = 0.95$  eV. In addition, a second, weaker, band is observed at higher energies, which is also attributed to  $9T^{2+\cdot}$ . After the addition of approximately two equivalents of  $\text{THI}^{+\cdot}\text{ClO}_4^-$  the absorption maximum of this band is found at  $E = 1.59$  eV. As was the case for 6T, the  $9T^{+\cdot} \rightarrow 9T^{2+\cdot}$  conversion produced a series of isosbestic points ( $E = 0.73, 1.32, 1.79,$  and  $2.37$  eV). The band at 0.82 eV is attributed to excitation of the doubly occupied HOMO level ( $b_2$ ) into the LUMO ( $a_2$ , the lowest bipolaron level) of the  $9T^{2+\cdot}$  dication (Theory section, Figure 2). In contrast to 6T, the onset of the formation of  $9T^{2+\cdot}$  can be observed in the UV/visible/near-IR spectrum before the band of 9T has bleached completely (Figure 9). This indicates that at intermediate oxidation levels a disproportionation equilibrium exists [Eq. (8)]. The coexistence of these three species is most



clearly observed in the second set of oxidation experiments (Figure 9, bottom) where the remainder of the neutral 9T absorption continues to decrease, while the  $9T^{2+\cdot}$  dication bands increase. A third weak absorption of  $9T^{+\cdot}$ , as observed for  $6T^{+\cdot}$  at 3.55 eV, could not be identified with certainty in the spectra; possibly it is part of the features seen in the spectra around the position of neutral 9T. Reduction with hydrazine monohydrate of the charged 9T oligomers shows that oxidation is fully reversible up to the dicationic state.

Carrying the oxidation process beyond the level of  $9T^{2+\cdot}$  results in a decrease of the band at  $E = 0.82$  eV, while a new absorption is found at  $E = 0.95$  eV (not shown). At these high oxidation levels, 9T is not stable, as we inferred by checking the reversibility with hydrazine monohydrate. For example, when the oxidation of 9T was continued until the absorption of unreacted  $\text{THI}^{+\cdot}$  appeared at  $E = 2.23$  eV in the UV/visible/near-IR spectrum, addition of an excess of hydrazine monohydrate gave a new hypsochromically shifted absorption band, which is attributed to a neutral oligothiophene (or polythiophene). The band maximum at  $E = 2.56$  eV suggests that on average three 9T units have coupled.<sup>[52]</sup> Because of these irreversible changes we did not investigate 9T in detail beyond the second oxidation stage.

Figure 10 shows the changes of the UV/visible/near-IR spectrum of  $9T^{+\cdot}$  with temperature in the range of  $T = 290$  to 230 K. Lowering the temperature results in a decrease of the  $9T^{+\cdot}$  bands at  $E = 0.67$  and 1.46 eV (labeled  $M_1$  and  $M_2$  in Figure 10) with a concomitant growth of two new bands at higher energy. In addition to an increasing intensity, the two new bands, labeled  $D_1$  and  $D_2$ , shift hypsochromically with decreasing temperature. Below  $T = 230$  K, however, their positions remain constant at  $E = 0.95$  and 1.94 eV, respectively. The observed temperature dependence is fully reversible

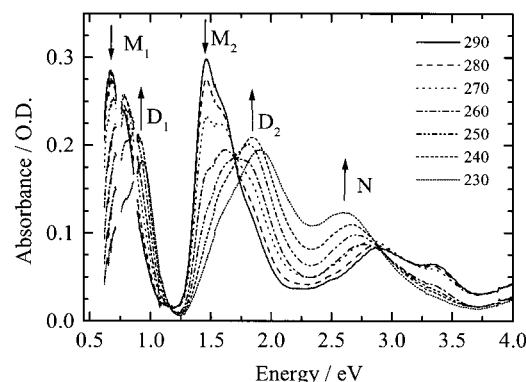


Figure 10. Temperature dependence of the UV/visible/near-IR spectra of the  $9T^{+\cdot}$  radical cation in a  $5 \times 10^{-6}$  M dichloromethane solution. Peaks labeled  $M_1$  and  $M_2$  are assigned to the monomeric  $9T^{+\cdot}$  radical cation, while  $D_1$  and  $D_2$  are attributed to their  $(9T^{2+\cdot})_2^+$   $\pi$  dimers. Band N is assigned to neutral 9T (see text). The temperature (K) is given in the inset.

and readily associated with the formation of  $\pi$  dimers of  $9T^{+\cdot}$  radical cations [Eq. (9)].



The dimerization is further corroborated by the decrease of the ESR signal in the same temperature range. The enthalpy of dimerization could not be determined accurately owing to extensive overlap of the electronic absorption bands of the radical cation and its dimer, but is estimated, and independently confirmed by temperature-dependent ESR experiments, to be  $\Delta H_{\text{dim}}^0 = -61 \pm 10$  kJ mol $^{-1}$ , that is, larger than the value for  $6T^{+\cdot}$ . The increase of the dimerization enthalpy with chain length is in accordance with published results.<sup>[15, 27]</sup> The changes that occur in the spectrum at the band labeled N (Figure 10), which increases in intensity and shifts bathochromically with decreasing temperature, are attributed to a thermochromic effect of neutral 9T. Like poly(3-alkylthiophenes), 9T forms microcrystallites at lower temperatures, causing a bathochromic shift of the absorption.<sup>[53]</sup> This phenomenon was confirmed independently by temperature-dependent UV/visible/near-IR spectroscopy on neutral 9T in which the same bathochromic shift is observed. Below  $T = 230$  K, the position of the band N remains constant at  $E = 2.60$  eV.

The ESR spectrum of  $9T^{+\cdot}$  in dichloromethane contains a single isotropic signal at  $g = 2.0023$  without any resolvable hyperfine coupling. The evolution of the ESR intensity with the amount of  $\text{THI}^{+\cdot}\text{ClO}_4^-$  added (Figure 7) reveals that the total amount of  $9T^{+\cdot}$  radical cations that can be present in solution is less than the total amount of  $6T^{+\cdot}$  radical cations formed under identical conditions. This result is consistent with the disproportionation equilibrium defined in Equation (8) because it explains the presence of diamagnetic species at intermediate oxidation levels. Likewise, the formation of  $\pi$  dimers according to Equation (9) can account for this result. The lower ESR signal observed for  $9T^{+\cdot}$  as compared to  $6T^{+\cdot}$  is consistent with the suggestion that the tendency to form  $\pi$  dimers of oligothiophene radical cations increases with conjugation length.<sup>[17, 27]</sup>



ESMS of 9T in dichloromethane solution, oxidized with one equivalent of  $\text{THI}^+\text{ClO}_4^-$ , produces the signals of  $9\text{T}^+$  at  $m/z = 1244.5$  and  $9\text{T}^{2+}$  at  $622.5$  amu, in accordance with the calculated mass of 9T ( $m/z = 1244.5$  amu) (Figure 11). In

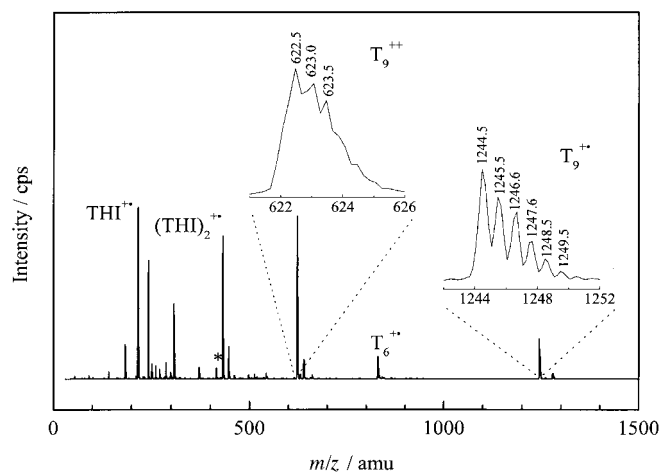


Figure 11. ES mass spectrum of a dichloromethane solution of the  $9\text{T}^+$  radical cation, which was fed directly into the ES mass spectrometer. The insets show expanded regions of interest (see text). The signals at  $m/z = 184.1$ ,  $216.1$ , and  $431.1$  amu are due to  $\text{THI}^+\text{-S}$ ,  $\text{THI}^+$ , and  $(\text{THI})_2^+$  respectively. The peak marked with an asterisk is attributed to  $6\text{T}^{2+}$  or  $9\text{T}^{3+}$  (see text). Small oligothiophene impurities are due to  $6\text{T}^+$  at  $m/z = 830.3$  amu and mono- $\alpha$ -chlorinated products of 9T at  $m/z = 1278.5$  amu ( $\alpha\text{-Cl-9T}^+$ ) and  $m/z = 639.5$  amu ( $\alpha\text{-Cl-9T}^{2+}$ ).<sup>[45]</sup> The peak at  $m/z = 242.5$  amu is due to the presence of a tetrabutylammonium contamination.

contrast to the mass spectra of 6T, which were recorded at the same intermediate oxidation level, the spectrum of 9T shows more doubly charged species than expected on the basis of the UV/visible/near-IR spectrum, demonstrating the different responsiveness in ESMS for the two 9T ions. Peaks attributable to  $(9\text{T})_2^+$  charge-transfer complexes or  $(9\text{T})_2^+$   $\pi$  dimers were not detected under these conditions. The isotope mass separations of the two 9T peaks are in full agreement with their single ( $m/z = 1244.5$  amu) and double charge ( $m/z = 622.5$  amu). For the peak at  $m/z = 1244.5$  amu this rules out important contributions from  $(9\text{T})_2^+$   $\pi$  dimers. At  $m/z = 414.3\text{--}416.6$  amu an unresolved peak is observed that could be due to either triply oxidized  $9\text{T}^{3+}$  (calcd  $m/z = 414.8$  amu) or an impurity of  $6\text{T}^{2+}$  (calcd  $m/z = 415.2$  amu). The presence of a small peak at  $m/z = 426.3$  amu of a triply charged mono- $\alpha$ -chlorinated by-product of 9T ( $\alpha\text{-Cl-9T}^{3+}$ , calcd  $m/z = 426.2$  amu), which is present as a by-product of the synthesis,<sup>[45]</sup> however, strongly suggests that  $9\text{T}^{3+}$  is formed under these conditions.

**Tetradodecyl duodecithiophene (12T):** The cyclic voltammogram of 12T ( $10^{-3}\text{M}$ ) recorded in dichloromethane shows a first oxidation wave at  $E^\circ = 0.59$  V with a separation between anodic and cathodic peaks of 50 mV (Figure 4c). The potential separation of less than 59 mV is most likely due to adsorption of charged 12T on the electrode. To check the possibility of aggregation effects of 12T on the cyclic voltammogram, we repeated the electrochemical measurements at a lower concentration ( $2 \times 10^{-4}\text{M}$ ), but obtained

identical results. Upon increasing the scan range, broad oxidation waves (peak-to-peak 80–100 mV) are observed around  $E = 0.82$  and  $0.98$  V. Increasing the voltage above  $E = 1.20$  V vs. SCE results in the formation of a new peak in the reduction wave at  $E = 0.37$  V with a simultaneous small decrease of the cathodic wave at  $0.57$  eV. This new peak could be the result of hysteresis in the reduction of charged species deposited on the electrode in the anodic scan.<sup>[54]</sup> A strong potential hysteresis is a common feature of solid-state voltammograms of many conjugated systems. In agreement with the present study, hysteresis effects in oligothiophenes are not observed until a certain potential or charging level is exceeded.<sup>[54]</sup>

The changes in the UV/visible/near-IR spectrum of 12T with increasing oxidation levels show marked differences from those for 6T and 9T (Figure 12). At the lowest oxidation

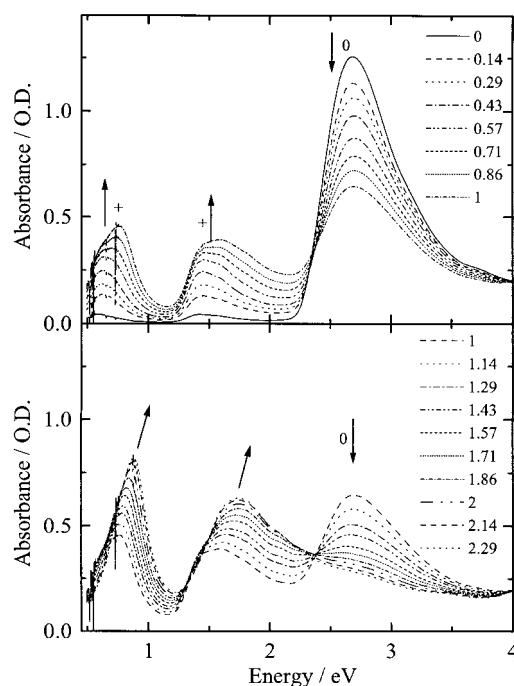


Figure 12. Evolution of the UV/visible/near-IR spectra of a  $1.2 \times 10^{-5}\text{M}$  solution of 12T in dichloromethane at  $T = 295$  K during conversion from neutral 12T to charged species. The top spectrum corresponds to the addition of the first equivalent of  $3 \times 10^{-4}\text{M}$  solution of  $\text{THI}^+\text{ClO}_4^-$  in dichloromethane, while the bottom spectrum represents the changes upon addition of the second equivalent. The inset shows the number of equivalents of  $\text{THI}^+\text{ClO}_4^-$  added.

levels two subgap absorptions are found at  $E = 0.59$  and  $1.42$  eV. Because  $12\text{T}^{2+}$  will be formed at the lowest oxidation levels, these two bands are readily assigned to the excitations from the highest doubly occupied level ( $a_u$ ) to the singly occupied polaron level ( $b_g$ ) and from this level to the empty polaron band ( $a_u$ , LUMO) (Figure 2). These bands shift slightly hypsochromically to  $E = 0.62$  and  $1.45$  eV after the addition of half an equivalent of  $\text{THI}^+\text{ClO}_4^-$  (Figure 12, top). Surprisingly, after the addition of exactly one equivalent of  $\text{THI}^+\text{ClO}_4^-$  the  $\pi\text{-}\pi^*$  absorption band of neutral 12T at  $E = 2.68$  eV has decreased to somewhat less than half its original intensity, indicating that neutral 12T is still present. This can

be explained by a disproportionation equilibrium of the kind described by Equation (10). Hence, at this stage of the oxidation,  $12T$ ,  $12T^{•+}$ , and  $12T^{2+}$  are simultaneously present in the solution, each to an appreciable extent.



During the addition of a second equivalent of  $THI^{•+}ClO_4^-$  the  $\pi-\pi^*$  absorption band continues to decrease (Figure 12, bottom), giving evidence of the further consumption of neutral  $12T$ . Simultaneously the two subgap absorption bands increase and the peaks exhibit a monotonous hypsochromic shift to  $E=0.88$  and  $1.75$  eV. The presence of two equally intense peaks at the doubly oxidized state is not compatible with a bipolaron structure, for which only one strong absorption is expected,<sup>[5, 22]</sup> but could be explained if two separated polarons were present on a chain. It is of interest to note that the energies of the two bands of  $12T^{2+}$  are close to those obtained for singly oxidized  $6T$  (Table 1).

Garnier et al. have recently suggested that for a slightly different  $12T$  derivative the doubly oxidized state in solution corresponds to a fourfold charged spinless  $\pi$  dimer,  $(12T)_2^{4+}$ , in which each molecule carries two noninteracting charges [Eq. (11)].<sup>[20]</sup> Each radical cation of this  $12T$  fourfold-charged



dication dimer is supposed to extend over approximately four thiophene units. Variable-temperature experiments may give evidence for the  $\pi$ -dimerization equilibrium of a doubly charged  $12T^{2+}$  molecule, similar to the temperature-induced dimerization of  $6T^{•+}$  and  $9T^{•+}$  [Eq. (12)]. Figure 13 shows the



variable temperature UV/visible/near-IR experiments of a solution of  $12T$  after oxidation with two equivalents of  $THI^{•+}ClO_4^-$  in chloroform (Figure 13a,  $T=290-330$  K) and dichloromethane (Figure 13b,  $T=190-295$  K). Cooling from ambient temperature to  $T=190$  K does not result in significant changes in the spectrum, apart from a small increase of the absorbance due to contraction of the solvent. Similarly, warming to  $T=330$  K only gives a decrease in absorbance. In contrast to cooling in dichloromethane, warming in chloroform is not completely reversible because of partial dedoping at higher temperatures. To summarize, no clear indication for an equilibrium as in Equation (12) could be obtained from these variable temperature UV/visible/near-IR experiments. Hence, no conclusive answer concerning the formation of  $(12T)_2^{4+}$   $\pi$  dimers from  $12T^{2+}$  can be given from the optical spectra, since the equilibrium appears to be entirely to the right hand or to the left hand of Equation (12) at all temperatures studied.

The UV/visible/near-IR spectra of  $12T$  recorded after addition of more than two equivalents of  $THI^{•+}ClO_4^-$  (Figure 14) reveal that the two bands at  $E=0.88$  and  $1.75$  eV diminish and are replaced by a new strong absorption which shifts slightly from  $E=1.10$  to  $1.18$  eV during the oxidation process. This band is assigned to higher oxidation products of

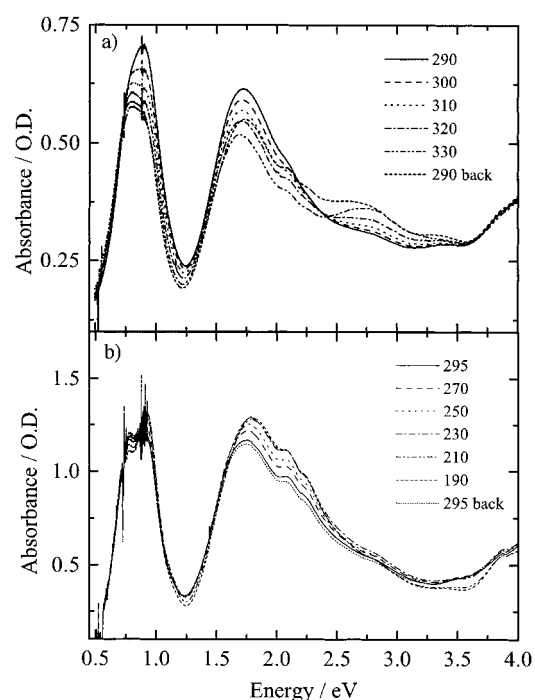


Figure 13. Temperature dependence of the UV/visible/near-IR spectra doubly oxidized  $12T$  in a  $1.2 \times 10^{-3}$  M dichloromethane solution (top) and in  $2.5 \times 10^{-5}$  M solution in chloroform (bottom). The temperature (K) is given in the key.

$12T$  such as triply charged ( $12T^{3+}$ ) and quadruply charged ( $12T^{4+}$ ) oligomers. Up to the dicationic state  $12T$  can be reduced reversibly to neutral  $12T$  by addition of hydrazine monohydrate. Reduction from higher oxidation levels results in a red shift of the  $\pi-\pi^*$  band.

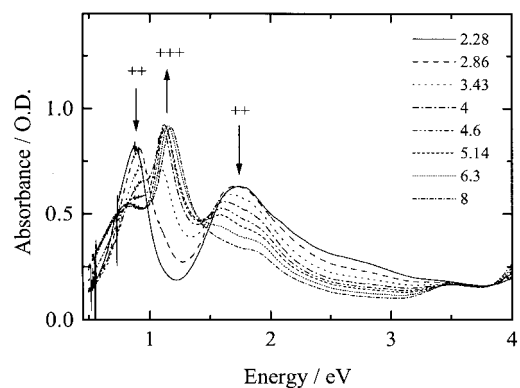


Figure 14. Evolution of the UV/visible/near-IR spectra of a  $1.2 \times 10^{-5}$  M solution of  $12T$  in dichloromethane at  $T=295$  K during conversion from doubly oxidized  $12T$  to higher charged species with a  $3 \times 10^{-4}$  M solution of  $THI^{•+}ClO_4^-$  in dichloromethane. The inset shows the number of equivalents of  $THI^{•+}ClO_4^-$  added.

Oxidation of  $12T$  in dichloromethane produces a weak isotropic ESR signal at  $g=2.0023$ , without any resolvable hyperfine coupling. Although a small increase in ESR intensity is observed after the addition of the first aliquot of  $THI^{•+}ClO_4^-$ , the total increase of the ESR spectrum during

progressive oxidation is negligible when compared with the experiments involving 6T and 9T (Figure 7). This observation is in full agreement with the disproportionation equilibrium proposed in Equation (10). When 12T is doubly oxidized in solution, the absence of an ESR spectrum at room temperature in solution does not rule out the possibility of a triplet state ( $12T^{2\cdot 2+}$ ). Lowering the temperature to  $T = 100$  K results in an increase of ESR intensity ( $I$ ) consistent with Curie's law ( $I = C/T$ ). Under these low-temperature conditions, a zero-field splitting or a signal at half field, characteristic for a triplet state in frozen solution, were not observed.

The ES mass spectrum of 12T (Figure 15) recorded after the addition of one equivalent of  $\text{THI}^{+\cdot}\text{ClO}_4^-$  reveals the presence of  $12T^{+}$ ,  $12T^{2+}$ , and  $12T^{3+}$  at  $m/z = 1658.7$ ,  $829.5$ , and  $553.5$  amu, respectively. High resolution MS of these peaks confirms the +1, +2, and +3 charge on these molecules. In particular the high-resolution mass spectrum of  $12T^{2+}$  shows a base peak at  $m/z = 829.5$  amu with a 0.5 amu isotope separation, which rules out the possibility that this manifold is due to  $6T^{+}$  (base peak at  $m/z = 830.3$  amu and unit mass separation). At  $m/z = 415$  amu a small peak is found, which can be attributed unambiguously to the quadruply charged  $12T^{4+}$  because an accompanying peak appears at  $m/z = 423.2$  from a mono- $\alpha$ -chlorinated 12T impurity ( $\alpha\text{-Cl-12T}^{4+}$ ).<sup>[45]</sup> Compared to the spectra of 6T and 9T, the relative intensity of the  $12T^{+}$  peak has further decreased in favor of higher charged ions, even when ES mass spectra were recorded at lower oxidation levels. It is important to note that the ES mass spectra of 12T recorded at various stages of the oxidation process do not show any evidence of  $\pi$  dimers of singly [ $(12T)_2^+$  calcd at  $m/z = 1658.6$  with 0.5 amu separation] or doubly [ $(12T)_2^{2+}$  calcd at  $m/z = 829.3$  with 0.25 amu separation] charged cations, nor any complexes thereof with a perchlorate anion.

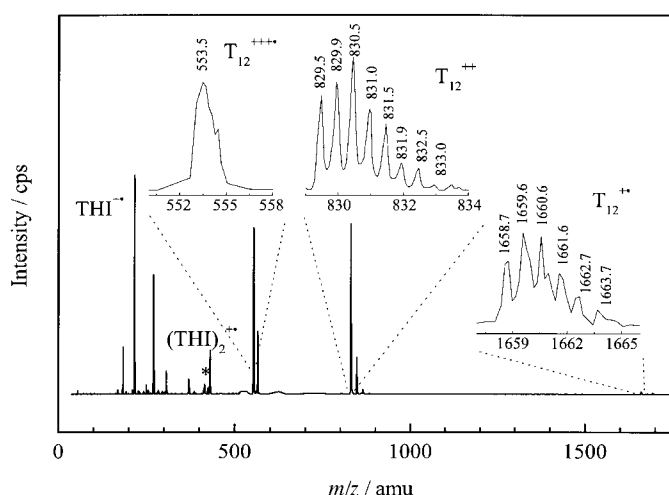


Figure 15. ES mass spectrum of a dichloromethane solution of 12T oxidized with one equivalent of  $\text{THI}^{+\cdot}\text{ClO}_4^-$  which was fed directly into the ES mass spectrometer. The insets show expanded regions of interest (see text). The line at  $m/z = 415$  amu marked with an asterisk is assigned to  $12T^{4+}$ . Oligothiophene impurities from mono- $\alpha$ -chlorinated products of 12T are found at  $m/z = 1692.6$  ( $\alpha\text{-Cl-12T}^{2+}$ ),  $846.5$  ( $\alpha\text{-Cl-12T}^{2+}$ ),  $565.2$  ( $\alpha\text{-Cl-12T}^{3+}$ ), and  $423.2$  amu ( $\alpha\text{-Cl-12T}^{4+}$ ).<sup>[45]</sup> The signals  $m/z = 184.1$ ,  $216.1$ , and  $431.1$  amu are due to  $\text{THI}^{+\cdot}\text{-S}$ ,  $\text{THI}^{+\cdot}$ , and  $(\text{THI})^{2+}$  respectively.

## Discussion

The experiments on 6T, 9T, and 12T demonstrate that within this homologous series 12T behaves quite differently from 6T or 9T. One of the salient differences is the observation that after addition of one equivalent of oxidizing agent ( $\text{THI}^{+\cdot}\text{ClO}_4^-$ ) to a solution of 12T, the optical absorption of the neutral 12T oligomer decreases only to approximately half the original intensity, while 6T and 9T are almost completely oxidized under similar conditions. This result confirms that the formation of a 12T dication is essentially a one-step reaction, as proposed by Horowitz et al. for a closely related tetrakis(decyl)-12T molecule.<sup>[19]</sup>

Another remarkable difference is found for the changes in the ESR intensity with increasing oxidation levels. For 6T and 9T, an increase, followed by a subsequent decrease, is observed when the oxidation is carried through the singly oxidized state, consistent with the formation of a radical cation ( $S = 1/2$ ) followed by its conversion to a dication with a bipolaronic structure ( $S = 0$ ). For 12T, the ESR signal, which is initially weak, hardly increases over the complete oxidation range, suggesting that the doubly charged state of 12T formed has no spin and corresponds to a bipolaron. However, the presence of two equally strong electronic subgap transitions strongly argues against the possible formation of bipolarons for 12T.<sup>[5, 22]</sup> We have performed semiempirical Hartree–Fock intermediate neglect of differential overlap (INDO) calculations coupled to a single configuration interaction (SCI) scheme. The results indicate that the absorption spectrum of 12T supporting a positive bipolaron is characterized by a single subgap feature owing to the selection rules imposed by the symmetry of the system. It might be argued that the charged defect is not necessarily localized in the central part of the oligomer, as typically obtained from geometry optimizations that preserve  $C_{2h}$  symmetry.<sup>[22, 55]</sup> However, a single subgap peak is also calculated for a 12T oligomer where the bipolaron is forced to be localized near one end of the chain. This is rationalized by the fact that the selection rules remain valid for the conjugated segment affected by the bipolaronic relaxation; the latter remains highly symmetric whatever the position of the center of the bipolaron. This is also the reason why alkyl side groups hardly modify the optical properties of doped conjugated chains. Note that a way to induce the appearance of a second subgap absorption in the spectrum is to generate two bipolarons in interaction on a single chain;<sup>[22]</sup> this feature is ruled out by the ESMS spectra on 12T but is a possibility in long polymer chains.

If it is not a bipolaron structure, what is the nature of that ESR-silent redox state in 12T? At this point, several interpretations are possible and it is important to address this issue in detail. The explanation advanced by Garnier et al. is that the  $12T^{2+}$  dication is present as a quadruply charged spinless  $\pi$  dimer in which each molecule carries two non-interacting charges.<sup>[20]</sup> As demonstrated in the preceding section, we have not been able to find proof for the existence of such a species using variable temperature UV/visible/near-IR absorption spectroscopy or ESMS. The absence of  $(12T)_2^{4+}$  mass peaks or any adduct thereof with  $\text{ClO}_4^-$  in the ES mass spectrum is significant in our view. We consider it unlikely that

$12T^{2+}$  has dimerized to a large extent, while going undetected in mass spectrometry, especially because  $\pi$  dimers were observed with ESMS for  $6T^{+}$  under conditions where dimerization has occurred to a small extent only. In addition, it is interesting to note that the optical transitions of  $(6T)_2^{2+}$  at 1.12 and 1.97 eV are significantly higher than the values obtained for  $12T_2^{2+}$  [or  $(12T)_2^{4+}$ ], 0.88 and 1.75 eV, respectively. It is thus unlikely that the spectrum of  $12T$  originates from a double  $\pi$  dimer formed by two noninteracting charges per chain.

Instead of a bipolaron or a  $\pi$  dimer,  $12T^{2+}$  might have a two-polaron electronic state. Both the bipolaron and the two-polaron states correspond to an  $^1A_g$  state, described by Equation (3), but the coefficients  $c_1$  and  $c_2$  differ: for a bipolaron  $c_1 \gg c_2$ , while for two polarons  $c_1 \approx c_2$ . The latter is in fact a diradical.<sup>[35]</sup> The ESR spectra of diradicals can vary strongly, depending on the strength of the exchange interaction  $J_0$  between the two electrons.<sup>[56]</sup> For very small exchange interactions, the ESR spectrum of a diradical is equivalent to that of two independent monoradicals. When the exchange interaction is small but significantly larger than the electron–nuclear hyperfine coupling ( $J_0 \gg a$ ), the ESR spectrum of the diradical exhibits a hyperfine splitting which is halved compared with that for the monoradical.<sup>[57, 58]</sup> For a conjugated system like  $12T$ , however, it is unlikely that the exchange interaction in a two-polaron state is small and corresponds to either of these two situations, because several electronic configurations interact. It is more likely that the diradical is in a singlet ground state with the  $^3B_u$  triplet state as a near-lying excited state.<sup>[59]</sup> A singlet state is of course ESR-silent. A triplet state should give an ESR signal in frozen solution where a characteristic anisotropic spectrum is expected, resulting from dipolar spin–spin interactions.<sup>[60]</sup> The experimental result that the  $12T$  dication does not show a triplet ESR signal in frozen solutions rules out the possibility that the triplet state is thermally populated. In this respect it is interesting to note that the dications of orthogonally bridged and spiro-fused phenylene–thiophene mixed oligomers were also found to produce no or very weak ESR signals under conditions where UV/visible/near-IR data suggest the presence of a single charge in each of the two orthogonal oligomer units.<sup>[61]</sup>

Therefore, based on all experimental results obtained from UV/visible/near-IR, ESR, and ESMS, we propose the most likely electronic configuration for the dication of  $12T$  is that of a  $^1A_g$  singlet ground state carrying two individual polarons, although direct spectral evidence for this proposition could not be obtained.

In Table 1, the optical transitions of the redox states of the  $nT$  ( $n = 6, 9, \text{ and } 12$ ) oligomers are listed together with the values reported for terthiophene.<sup>[62]</sup> Figure 16 reveals that for the neutral oligomers ( $nT$ ) and the singly oxidized radical cations ( $nT^{+}$ ) an approximate linear relation is observed between the peak position ( $h\nu_{\max}$ ) and the reciprocal of the number of thiophene rings ( $1/n$ ) in the oligomer. This approximate linear behavior is characteristic of many  $\pi$ -conjugated oligomers and their redox states but is found to break down for longer neutral oligomers, where values at higher energies are found, resulting in a curve.<sup>[28, 63]</sup> Figure 16

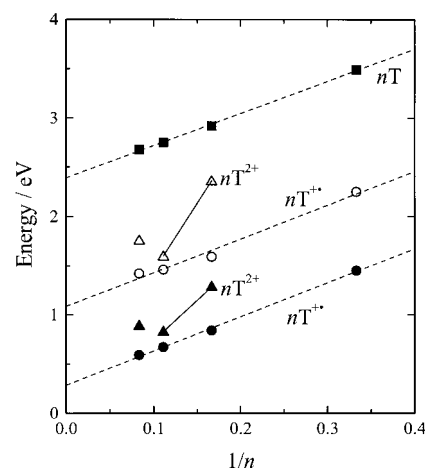


Figure 16. Evolution of the peak positions observed in the UV/visible/near-IR spectra as function of  $1/n$  for the neutral (■); radical cation (●, ○); and dication (▲, △) redox states of oligothiophenes  $nT$  ( $n = 3, 6, 9, \text{ and } 12$ ).

Table 1. UV/visible/near-IR data of the redox states of the  $nT$  oligomers ( $h\nu_{\max}$  (eV)).

Oligomer	Neutral	Radical cation		$\pi$ Dimer		Dication	
		1	2	1	2	1	2
3 <sup>[a]</sup>	3.50	1.46	2.25				
6	2.92	0.84	1.59	1.12	1.97	1.28	2.35 <sup>[b]</sup>
9	2.75	0.67	1.46	0.95	1.94	0.82	1.59
12	2.68	0.59 <sup>[c]</sup>	1.42 <sup>[c]</sup>			0.75 <sup>[d]</sup>	1.60 <sup>[d]</sup>
						0.88 <sup>[e]</sup>	1.75 <sup>[e]</sup>

[a] Data for  $3T$  were taken from ref. [62]. [b] Very weak transition. [c] Peak position at the initial stages of oxidation. [d] Peak position after addition of 1 equiv. of oxidant. [e] Peak position after addition of 2 equiv. of oxidant.

shows that this also seems true for the electronic transitions of the radical cations, although the limited number of points does not allow a firm conclusion. From Figure 16 it can be seen that the bathochromic shift of the bands with  $1/n$  is found to be similar for the neutral and singly oxidized states, in full accordance with previous results.<sup>[15, 18a, 19, 27]</sup> The slope of these lines is about  $3.4 \pm 0.15$  eV. For the dications, the situation is different. Previous studies on shorter oligothiophenes have shown that the most prominent dication absorption band also shifts linearly to lower energies with  $1/n$ , but with a much steeper slope ( $6.0 \pm 0.5$  eV).<sup>[15, 18a, 19]</sup> Figure 16 reveals that this behavior is also observed for the strong bipolaron transition of the  $6T^{2+}$  and  $9T^{2+}$  dications. It is noteworthy that even the weak absorption bands at higher energies of  $6T^{2+}$  and  $9T^{2+}$  dications follow the same trend. Figure 16 clearly demonstrates the different electronic structure of the  $12T^{2+}$  dication when compared to the shorter oligomers, giving an unexpected increase in transition energies with increasing  $n$ . The important conclusion is that the absorption bands of  $12T^{2+}$  are not found at the energies expected for a bipolaronic structure.

## Conclusion

We have presented a detailed study on the redox states of long oligothiophenes ( $6T$ ,  $9T$ , and  $12T$ ) using UV/visible/near-IR in combination with ESR spectroscopy and electrospray mass

spectrometry. Radical cations (polarons),  $\pi$  dimers of radical cations, and dications with a closed-shell structure (bipolarons) have been characterized for 6T and 9T. The most interesting results have been obtained for the longest oligothiophene (12T), which behaves completely differently from the shorter homologues. The electronic structure of the 12T<sup>2+</sup> dication is not in accordance with the expected features of a bipolaron, and we propose that it is in a singlet state carrying two individual polarons. Such behavior has been recently predicted based on theoretical calculations.<sup>[31]</sup> The rationale for this effect in dications of oligothiophenes is that the decrease in Coulomb repulsion obtained by moving the two positive polarons further apart along the chain outweighs the energy cost required for creating two individual geometry deformations on the chain, instead of a single deformation associated with a bipolaron.

Our results demonstrate that for a long oligomer (or an infinite polymer) new states may occur that cannot be found in short oligomers because the restricted length disfavors such a configuration. We might actually expect the relative stability of one bipolaron versus two polarons to result from a fine balance depending intimately on the experimental conditions, such as solvent and type of counterions.<sup>[64]</sup>

## Experimental Section

The oligothiophenes used in this study were synthesized by Syncom B.V., Groningen (The Netherlands). The solubilizing dodecyl (d) side chains of the oligothiophenes are substituted on the  $\beta$  positions of every third thiophene ring, starting at the second ring (i.e. 6T = (2,5)d<sub>2</sub>-6T; 9T = (2,5,8)d<sub>3</sub>-9T; 12T = (2,5,8,11)d<sub>4</sub>-12T). Their synthesis involved the oxidative coupling of  $\alpha$ -lithiooligothiophenes with cupric chloride. Details of their preparation will be published elsewhere.<sup>[65]</sup> The mass spectra and elemental analysis are consistent with the proposed structures (see analytical data below). All oxidation experiments were performed under an inert N<sub>2</sub> atmosphere (<1 ppm H<sub>2</sub>O and <10 ppm O<sub>2</sub>). Commercial-grade solvents were purified, dried, and deoxygenated following standard methods. Cyclic voltammograms were recorded with 0.1 M tetrabutylammonium hexafluorophosphate (TBAH) as supporting electrolyte with a Potentiostat Wenking POS 73 potentiostat. Substrate concentration was typically 10<sup>-3</sup> M. The working electrode was a platinum disc (0.2 cm<sup>2</sup>), the counterelectrode was a platinum plate (0.5 cm<sup>2</sup>), and a saturated calomel electrode was used as reference electrode, calibrated against a Fc/Fc<sup>+</sup> couple (+0.470 V vs. SCE). UV/visible/near-IR experiments were performed with a Perkin Elmer Lambda 900 spectrophotometer equipped with an Oxford Optistat cryostat and ITC 502 controller for variable temperature experiments down to 80 K. The typical concentration in optical experiments was 10<sup>-5</sup> M. ESR experiments were carried out with an X-band Bruker ESP 300E spectrometer, operating with a standard or TMH cavity, an ER 035 M NMR Gauss meter, and a HP 5350 B frequency counter. Temperature was controlled by means of a Bruker ER 4111 variable-temperature unit. Combined UV/visible/near-IR and ESR studies were performed with a home-made cell consisting of a 10 mm quartz cuvette, a quartz 4 mm o.d. ESR tube, and a teflon-lined septum-sealed entry port for addition of oxidizing agent through a gas-tight Hamilton syringe. Electro spray mass spectra were recorded with a Perkin Elmer Sciex API 300 MS/MS mass spectrometer. The sample solutions were delivered to the ESMS by a syringe pump (Harvard Apparatus) at a flow rate of  $\approx 5 \mu\text{L min}^{-1}$ . Under the conditions applied for ESMS, injection of neutral oligothiophenes did not give detectable signals of oxidized species. MS–MS spectra revealed that fragmentation only occurs to a small extent, giving benzylic fission leading to loss of C<sub>11</sub>H<sub>23</sub> (155.2 amu) fragments.

## Analytical data:

**(2,5)d<sub>2</sub>-6T:** EI-MS:  $m/z$  ( $M^{+}$ ): calcd 830.32; obs 830.5; anal. calcd for C<sub>48</sub>H<sub>62</sub>S<sub>6</sub>: C 69.35, H 7.52, S 23.14; found: C 69.25, H 7.51.

**(2,5,8)d<sub>3</sub>-9T:** EI-MS:  $m/z$  ( $M^{+}$ ): calcd 1244.47; obs 1244.5; anal. calcd for C<sub>72</sub>H<sub>92</sub>S<sub>9</sub>: C 69.40, H 7.44, S 23.16; found: C 69.39, H 7.53.

**(2,5,8,11)d<sub>4</sub>-12T:** EI-MS:  $m/z$  ( $M^{+}$ ): calcd 1658.62; obs 1658.7; anal. calcd for C<sub>96</sub>H<sub>122</sub>S<sub>12</sub>: C 69.43, H 7.40, S 23.17; found: C 69.39, H 7.37.

**Acknowledgments:** We are grateful to Philips Research for an unrestricted research grant supporting these investigations and for generously providing the oligothiophenes used in this study. Furthermore we wish to thank Dr. A. J. W. Tol (Philips Research), Dr. W. ten Hoeve (Syncom B.V.), Prof. E. W. Meijer, and Dr. M. M. Wienk (EUT) for stimulating discussions, and B. A. J. Jansen for his assistance in parts of the project. The work in Mons is partly supported by the Belgian Federal Government Services for Scientific, Technical, and Cultural Affairs (Interuniversity Attraction Pole in Supramolecular Chemistry and Catalysis), FNRS-FRFC, and an IBM Academic Joint Study. The Eindhoven–Mons collaboration is carried out in the framework of the European Commission Training and Mobility of Researchers Network SELOA. J.C. is Chargé de Recherches of the Belgian National Fund for Scientific Research.

Received: November 18, 1997 [F897]

- [1] *Handbook of Organic Conductive Molecules and Polymers, Vols. 1–4* (Ed.: H. S. Nalwa), Wiley, New York, **1997**.
- [2] *Handbook of Conducting Polymers*, 2nd ed. (Eds.: T. A. Skotheim, J. R. Reynolds, R. L. Elsenbaumer), Marcel Dekker, New York, **1997**.
- [3] W. P. Su, J. R. Schrieffer, A. J. Heeger, *Phys. Rev. Lett.* **1979**, *42*, 1698; *Phys. Rev. B* **1980**, *22*, 2099.
- [4] S. A. Brazovskii, N. N. Kirova, *Sov. Phys. JETP Lett.* **1981**, *33*, 4.
- [5] K. Fesser, A. R. Bishop, D. K. Campbell, *Phys. Rev. B* **1983**, *27*, 4804.
- [6] J. L. Brédas, G. B. Street, *Acc. Chem. Res.* **1985**, *18*, 309.
- [7] A. J. Heeger, S. Kivelson, J. R. Schrieffer, W. P. Su, *Rev. Mod. Phys.* **1988**, *60*, 781.
- [8] O. A. Patil, A. J. Heeger, F. Wudl, *Chem. Rev.* **1988**, *88*, 183.
- [9] Y. Furukawa, *J. Phys. Chem.* **1996**, *100*, 15644.
- [10] In chemical terminology a *positive polaron* (which is an expression used in solid-state physics) corresponds to a *radical cation*, associated to a local geometry relaxation; see ref. [6].
- [11] A *bipolaron* is a pair of like charges with an associated strong local geometry deformation; see ref. [6].
- [12] Furukawa (ref. [9]) has estimated the expected intensity ratio of the two subgap absorptions for polythiophene based on FBC theory (ref. [5]) to be about 14, in sharp contrast with the observed ratio of about 1.2.
- [13] a) D. Fichou, B. Xu, G. Horowitz, F. Garnier, *Synth. Met.* **1991**, *41–43*, 463; b) D. Fichou, G. Horowitz, F. Garnier, *Synth. Met.* **1990**, *39*, 125; c) D. Fichou, G. Horowitz, B. Xu, F. Garnier, *Synth. Met.* **1990**, *39*, 243.
- [14] a) M. G. Hill, K. R. Mann, L. L. Miller, J.-F. Penneau, *J. Am. Chem. Soc.* **1992**, *114*, 2728; b) M. G. Hill, J.-F. Penneau, B. Zinger, K. R. Mann, L. L. Miller, *Chem. Mater.* **1992**, *4*, 1106.
- [15] P. Bäuerle, U. Segelbacher, A. Maier, M. Mehring, *J. Am. Chem. Soc.* **1993**, *115*, 10217.
- [16] a) D. D. Graf, J. P. Campbell, L. L. Miller, K. R. Mann, *J. Am. Chem. Soc.* **1996**, *118*, 5480; b) D. D. Graf, R. G. Duan, J. P. Campbell, L. L. Miller, K. R. Mann, *J. Am. Chem. Soc.* **1997**, *119*, 5888.
- [17] P. Bäuerle, U. Segelbacher, K.-U. Gaudl, D. Huttenlocher, M. Mehring, *Angew. Chem.* **1993**, *105*, 125; *Angew. Chem. Int. Ed. Engl.* **1993**, *32*, 76.
- [18] a) J. Guay, P. Kasai, A. Diaz, R. Wu, J. M. Tour, L. H. Dao, *Chem. Mater.* **1992**, *4*, 1097; b) J. Guay, A. Diaz, R. Wu, J. M. Tour, L. H. Dao, *Chem. Mater.* **1992**, *4*, 254.
- [19] G. Horowitz, A. Yassar, H. J. Von Bardeleben, *Synth. Met.* **1994**, *62*, 245.
- [20] B. Nessakh, G. Horowitz, F. Garnier, F. Deloffre, P. Srivastava, A. Yassar, *J. Electroanal. Chem.* **1995**, *399*, 97.
- [21] J. Cornil, J. L. Brédas, *Adv. Mater.* **1995**, *7*, 295.
- [22] J. Cornil, D. Beljonne, J. L. Brédas, *J. Chem. Phys.* **1995**, *103*, 842.

- [23] Detailed investigations of the influence of the solvent and solvent polarity on the dimerization enthalpy of radical cations are in progress.
- [24] L. L. Miller, K. R. Mann, *Acc. Chem. Res.* **1996**, *29*, 417.
- [25] J. A. E. H. van Haare, L. Groenendaal, E. E. Havinga, R. A. J. Janssen, E. W. Meijer, *Angew. Chem.* **1996**, *108*, 696; *Angew. Chem. Int. Ed. Engl.* **1996**, *35*, 638.
- [26] A. Sakamoto, Y. Furukawa, M. Tasumi, *J. Phys. Chem. B* **1997**, *101*, 1726.
- [27] Y. Yu, E. Gunic, B. Zinger, L. L. Miller, *J. Am. Chem. Soc.* **1996**, *118*, 1013.
- [28] P. Bäuerle, T. Fisher, B. Bidlingmeier, A. Stabel, J. P. Rabe, *Angew. Chem.* **1995**, *107*, 335; *Angew. Chem. Int. Ed. Engl.* **1995**, *34*, 303.
- [29] M. Sato, M. Hiroi, *Polymer* **1996**, *37*, 1685.
- [30] It is also possible to rationalize this by stating that the energy required to remove an electron from a fragment of a long chain which already carries a charge is higher than the energy needed to remove the electron from a neutral part of the same chain.
- [31] a) A. J. W. Tol, *Chem. Phys.* **1996**, *208*, 73; b) A. J. W. Tol, *Synth. Met.* **1995**, *74*, 95.
- [32] P. Kebarle, L. Tang, *Anal. Chem.* **1993**, *65*, 772A.
- [33] In the discussion, we only consider  $C_{2h}$  ( $n$  even), but the conclusions are fully analogous for  $C_{2v}$  ( $n$  odd). For  $C_{2v}$  the labels  $b_g$  and  $a_u$  have to be replaced by  $a_2$  and  $b_2$ , respectively.
- [34] Examples can be found for oligothiophenes in ref. [13], for oligopyrroles in ref. [25], and for oligo( $p$ -phenylene vinylene)s see: M. Deussen, H. Bässler, *Chem. Phys.* **1992**, *164*, 247.
- [35] Here we define a diradical a molecule as one in which two electrons occupy two degenerate or nearly degenerate molecular orbitals. *Angew. Chem.* **1972**, *84*, 86; L. Salem, C. Rowland, *Angew. Chem. Int. Ed. Engl.* **1972**, *11*, 92.
- [36] W. T. Borden in *Diradicals* (Ed.: W. T. Borden), John Wiley, New York, **1982**, pp. 1–72.
- [37] The relative energies of these four states, considering only the MOs  $\phi_+$  and  $\phi_-$ , are given by the following equations (see: A. Szabo, N. S. Ostlund, *Modern Quantum Chemistry*, McGraw–Hill, New York, **1989**):
- $${}^1A_g \quad E_1 = h_{++} + h_{--} + \frac{J_{++} + J_{--}}{2} - \left[ K_{+-}^2 + \left( h_{--} - h_{++} + \frac{J_{--} - J_{++}}{2} \right)^2 \right]^{1/2}$$
- $${}^2A_g \quad E_2 = h_{++} + h_{--} + \frac{J_{++} + J_{--}}{2} + \left[ K_{+-}^2 + \left( h_{--} - h_{++} + \frac{J_{--} - J_{++}}{2} \right)^2 \right]^{1/2}$$
- $${}^1B_u \quad E_3 = h_{++} + h_{--} + J_{+-} - K_{+-}$$
- $${}^1B_u \quad E_4 = h_{++} + h_{--} + J_{+-} + K_{+-}$$
- [38] Note that  $K_{+-}$  will not converge to zero, even in the limit of a negligible interaction between the two radical cation wavefunctions  $\phi_+$  and  $\phi_-$ . Substitution of Equations (1) and (2) in the expression for  $K_{+-} = \langle \phi_+ \phi_- | r^{-1} | \phi_- \phi_+ \rangle$  gives for  $r_{AB} \rightarrow \infty$ :  $K_{+-} = 1/4 (\langle \phi_A \phi_A | r^{-1} | \phi_A \phi_A \rangle + \langle \phi_B \phi_B | r^{-1} | \phi_B \phi_B \rangle) \neq 0$ .
- [39] A. J. Bard, L. R. Faulkner, *Electrochemical Methods*, John Wiley, New York, **1980**, p. 702.
- [40] H. J. Shine, C. F. Dais, R. Small, *J. Org. Chem.* **1964**, *29*, 21.
- [41] R. A. J. Janssen, D. Moses, N. S. Sariciftci, *J. Chem. Phys.* **1994**, *101*, 9519.
- [42] a) J. Poplawski, E. Ehrenfreund, J. Cornil, J. L. Brédas, R. Pugh, M. Ibrahim, A. J. Frank, *Mol. Cryst. Liq. Cryst.* **1994**, *256*, 407; b) G. Lanzani, L. Rossi, A. Piaggi, A. J. Pal, C. Taliani, *Chem. Phys. Lett.* **1994**, *226*, 551; c) R. A. J. Janssen, M. P. T. Christiaans, K. Pakbaz, D. Moses, J. C. Hummelen, N. S. Sariciftci, *J. Chem. Phys.* **1995**, *102*, 2628; d) P. A. Lane, X. Wei, Z. V. Vardeny, *Phys. Rev. Lett.* **1996**, *77*, 1544.
- [43] M. G. Harrison, R. H. Friend, F. Garnier, A. Yassar, *Synth. Met.* **1994**, *67*, 215.
- [44] J. Cornil, D. Beljonne, J. L. Brédas, *J. Chem. Phys.* **1995**, *103*, 834.
- [45] Small amounts of  $\alpha$ -chlorinated by-products are known to be formed during the oligomer synthesis in the oxidative coupling reaction of the  $\alpha$ -lithio derivatives with cupric chloride. See: a) H. E. Katz, L. Torsi, A. Dodabalapur, *Chem. Mater.* **1995**, *7*, 2235; b) H. E. Katz, L. Torsi, A. Dodabalapur, A. J. Lovinger, R. Ruel, *Polym. Mater. Sci. Eng.* **1995**, *72*, 467.
- [46] The possibility that this peak results from a  $12T^{+}$  impurity has been discarded because  $12T^{+}$  is expected at  $m/z = 1658.6$  amu, i.e. 2 amu less than observed.
- [47] a) B. Badger, B. Brocklehurst, *Trans. Farad. Soc.* **1969**, *65*, 2576; b) A. Tsuchida, M. Yamamoto, *J. Photochem. Photobiol. A Chem.* **1992**, *65*, 53.
- [48] a) S. Hotta, K. Waragai, *J. Phys. Chem.* **1993**, *97*, 7427; b) K. Tanaka, Y. Matsuura, Y. Oshima, T. Yamabe, S. Hotta, *Synth. Met.* **1994**, *66*, 295.
- [49] In ref. [17] the high-energy band of the  $(6T)_2^+$   $\pi$  dimer is found at  $E = 1.81$  eV, coinciding with a vibronic replica of the high-energy band of  $6T^+$ . Below temperatures of  $T = 240$  K, however, we observe that a band at  $E = 1.97$  eV increases and becomes the strongest absorption of the  $(6T)_2^+$   $\pi$  dimer, while the band at  $E = 1.81$  eV evolves into a shoulder.
- [50] The exact origin of this discrepancy is unclear. The only difference between the two experiments is that Bäuerle et al.<sup>[17]</sup> used one regioisomer of 6T (i.e., 3''',4'-didodecyl-2,2':5,2'':5'',2''':5''',2''''-sexithiophene) while in this study the dodecyl side chains on the second and fifth thiophene ring are either at the 3 or the 4 position, resulting in a mixture of three regioisomers, (3',4'''), (3',3'''), and (3''',4'')-dodecyl, for 6T.
- [51] *Electroanalytical Chemistry, Vol. 14* (Ed.: A. J. Bard), Marcel Dekker, New York, **1986**.
- [52] From a parabolic fit of the data of 3T ( $E = 3.57$  eV), 6T, 9T, and 12T the relation  $E = 4.09/n^2 + 1.86/n + 2.49$  eV is obtained for the absorption maximum of neutral  $nT$ , which gives  $n \approx 31$  when  $E = 2.56$  eV.
- [53] S. D. D. V. Rugooputh, S. Hotta, A. J. Heeger, F. Wudl, *Polym. Sci. Polym. Phys. Ed.* **1987**, *25*, 1071.
- [54] K. Meerholz, J. Heinze, *Electrochim. Acta* **1996**, *41*, 1839.
- [55] C. Ehrendorfer, A. Karpfen, *J. Phys. Chem.* **1994**, *98*, 7492.
- [56] To a first approximation the isotropic coupling constant  $J_0$ , which describes the electron exchange interaction by the Hamiltonian  $\hat{H}_{ex} = -2J_0 \hat{S}_1 \cdot \hat{S}_2$ , is identical to the exchange integral  $K_{AB}$  of the two singly occupied MOs carrying the unpaired electrons.
- [57] G. R. Luckhurst in *Spin Labeling Theory and Applications* (Ed.: L. Berliner), Academic Press, New York, **1976**, p. 133.
- [58] The largest hyperfine coupling of the  $6T^+$  radical cation amounts to about 0.2 mT (Figure 6) so that the exchange interaction  $J_0$  can be less than  $20 \text{ MJ mol}^{-1}$  (or  $2 \times 10^{-7}$  eV) to still give the diradical spectrum. Clearly this is much less than the thermal energy.
- [59] a) M. M. Glasbeek, J. D. W. van Voorst, G. J. Hoijtink, *J. Chem. Phys.* **1996**, *45*, 1852; b) F. Kanno, K. Inoue, N. Koga, H. Iwamura, *J. Am. Chem. Soc.* **1993**, *115*, 847; c) M. Dvolaitzky, R. Chirarelli, A. Rassat, *Angew. Chem.* **1992**, *104*, 220; *Angew. Chem. Int. Ed. Engl.* **1992**, *31*, 180; d) U. Müllen, M. Baumgarten, *J. Am. Chem. Soc.* **1995**, *117*, 5840.
- [60] A. Carrington, A. D. McLachlan, *Introduction to Magnetic Resonance*, Chapman and Hall, London, **1967**.
- [61] J. R. Diers, M. K. DeArmond, J. Guay, A. Diaz, R. Wu, J. S. Schumm, J. M. Tour, *Chem. Mater.* **1994**, *6*, 327.
- [62] V. Wintgens, P. Valat, F. Garnier, *J. Phys. Chem.* **1994**, *98*, 228.
- [63] H. Meier, U. Stalmach, H. Kolshorn, *Acta Polym.* **1997**, *48*, 379.
- [64] S. Irle, H. Lischka, *J. Chem. Phys.* **1997**, *107*, 3021.
- [65] W. Ten Hoeve, H. Wynberg, unpublished results.